The Othmer-Tobias relationship is frequently expressed in wt % rather than mol %, but in the systems of these acids with furfural and water the latter may be linear even though the former may not be (*5*). Figure 2 shows that for the valeric acid system, the latter is also nonlinear. Moreover it is branched and passes through an extreme abscissa. Data are insufficient to establish whether the extreme involves a continuous or discontinuous first derivative of the function. The Hand relationship in Figure 2 shows a similar behavior.

The relationship of Bachman is linear in Figure 2, with a slope and intercept by a least-squares procedure of, respectively, 91.53 and −0.37. Clearly this relationship is the most useful of the three in that the maxima of the binodal curve, Figure 1, do not affect the continuity of the tie-line correlation.

For each of the three plots of Figure 2, the points corresponding to the maxima in Figure 1 have been added. That point is consistent with the linearity of the Bachman plot, and lies on one of the branches of each of the other two plots.

The effectiveness of the extraction of a solute by a solvent is given by the selectivity (*10*), which in the present work may be considered as the ability of furfural to separate water and acid. Then the selectivity may be defined here as either b_2c_1/b_1c_2 or the equivalent ratio B_2C_1/B_1C_2. The selectivities in the valeric acid system at 25° and 35°C, and of the other acid systems at 25°C are given in Figure 3. The selectivity is greatest in the valeric acid system, and this system exhibits a selectivity minimum at the coexistent maxima of the binodal curves. Figure 3 shows that the effect of temperature in the present system is relatively small.

LITERATURE CITED

(1) Bachman, I., *Ind. Eng. Chem., Anal. Ed.*, **12**, 38 (1940).
(2) Dreisbach, R. R., *Advan. Chem. Ser.*, No. 29, 439 (1961).
(3) Hand, D. B., *J. Phys. Chem.*, **34**, 1961 (1930).
(4) Heric, E. L., Blackwell, B. H., Gaissert, L. J., III, Grant, S. R., Pierce, J. W., *J. Chem. Eng. Data*, **11**, 38 (1966).
(5) Heric, E. L., Rutledge, R. M., *ibid.*, **5**, 272 (1960).
(6) Langford, R. E., Heric, E. L., *ibid.*, **17**, 87 (1972).
(7) Othmer, D. F., Tobias, P. E., *Ind. Eng. Chem.*, **34**, 693 (1942).
(8) Quaker Oats Co., *Bull. 203-B*, p 4, Chicago, 1968.
(9) Skrzec, A. E., Murphy, N. F., *Ind. Eng. Chem.*, **46**, 2245 (1954).
(10) Treybal, R. E., "Liquid Extraction," 2nd ed., p 43, McGraw-Hill, New York, N. Y., 1963.

RECEIVED for review October 12, 1971. Accepted November 13, 1971

Examination of Ethanol–*n*-Heptane, Methanol–*n*-Hexane Systems Using New Vapor-Liquid Equilibrium Still

J. DAVID RAAL,[1] RUSSEL K. CODE, and DONALD A. BEST
Queen's University, Kingston, Ont., Canada

Isobaric vapor-liquid equilibrium data are presented for the binary systems ethanol–*n*-heptane and methanol–*n*-hexane. Rigorous thermodynamic tests indicated excellent thermodynamic consistency. The data were obtained using a new dynamic vapor-liquid equilibrium still. A salient feature of the design is a two-phase vapor-liquid flow through an annular space surrounding the equilibrium chamber which permits accurate temperature measurement and ensures adiabatic operation of the inner chamber at thermal equilibrium.

The two binary systems examined were ethanol–*n*-heptane and methanol–*n*-hexane. Both systems are highly nonideal, and the relative volatilities, particularly in the hydrocarbon-rich regions, are very large. Accurate determination of vapor-liquid equilibrium data for such systems presents a stringent test of the experimental method. Also, the availability of heat of-mixing data permits rigorous testing of the data for thermodynamic consistency. Equilibrium data predicted by Van Ness et al. (*18*) from total pressure–composition measurements show a maximum in one of the activity coefficient–composition curves. Such a maximum was not detected (*9*).

Isobaric vapor-liquid equilibrium data were determined for the above two systems using a new dynamic vapor-liquid equilibrium still described in detail below.

EQUILIBRIUM STILL DESIGN

Among the more serious difficulties encountered with many of the equilibrium stills presented in the literature (*4*) are partial condensation of the equilibrium vapor (which may lead to considerable error), inadequate mixing and vapor-liquid contact in the equilibrium chamber, complete evaporation of liquid droplets, and imprecise temperature measurement.

An attractive feature of stills with vapor-phase circulation of the kind proposed by Jones-Colburn (*7*) is the excellent mixing and intimate contact of vapor bubbles with surrounding liquid in the equilibrium chamber. Drawbacks of this design (and its subsequent modifications) are the imprecise measurement of boiling temperature and the difficulties encountered in exactly balancing heat losses to maintain adiabatic operation of the equilibrium chamber. Also, vertical temperature gradients in the latter, such as may arise from uneven heating, may produce erroneous results.

The above drawbacks are largely eliminated in stills with circulation of both liquid and vapor phases of the type proposed by Gillespie (*3*) and subsequently modified by several investigators (*1*, *2*, *13*). The Cottrell pump feature of these stills permits very precise temperature measurement but provides less satisfactory mixing and vapor-liquid contact than the bubbling chamber of the Jones still. Partial condensation of equilibrium vapor, although very effectively reduced, probably is not completely eliminated particularly in the region of the thermocouple

[1] To whom correspondence should be addressed.

well. The rather long times required to reach steady state is somewhat unsatisfactory.

In the still described below, the efficient mixing characteristics of the Jones-Colburn design are combined with a novel adaptation of the Cottrell pump to provide accurate temperature measurement and to ensure adiabatic operation of the equilibrium chamber at all operating temperatures.

The design is shown in Figure 1. The inner equilibrium chamber, A, fits closely inside the outer jacket, B. Liquid heated in the lower portion of B by the electrical resistance windings, R, forms vapor bubbles so that the annular space between A and B acts as a Cottrell pump, propelling a mixture of vapor and liquid onto the jacketed thermocouple, T, while maintaining the inner chamber at the temperature of the boiling liquid. The vapor separates from the liquid in the inner downcomer, C, following the path indicated in the diagram, and bubbles through the liquid in the inner equilibrium chamber. The vapor passes through the superheated section, H, is condensed, and flows through the magnetically stirred sample trap, S, before returning to the heated section. Superheating and bumping of liquid in the heated section are prevented by introducing a slow stream of fine dry air bubbles through the capillary D. (Dry nitrogen may be used to prevent oxidation of the contents where necessary.) The bubbles impinge on the shield, K, and are directed into the outer tube, probably assisting somewhat in the mixing of returning condensate with liquid in the zone above stopcock S_1.

To prevent partial condensation of vapor in the space surrounding the thermocouple, T, the upper portions of the apparatus are lagged with suitable insulating material, as shown. Elimination of vapor condensation in this region and effective heat transfer between the inner and outer chambers should ensure equalization of composition in the two regions at equilibrium. For the two binary systems studied in the present work, liquid in the inner and outer chambers (i.e., A, B) invariably reached the same composition at equilibrium. Liquid samples should, however, be taken from the inner chamber since there is no danger of incomplete mixing of returning condensate or cooling of the equilibrium vapor. The pressure in the outer chamber is slightly higher than that in the vapor space in A. For most precise temperature measurement a correction may be applied by considering the hydrostatic head of liquid in A.

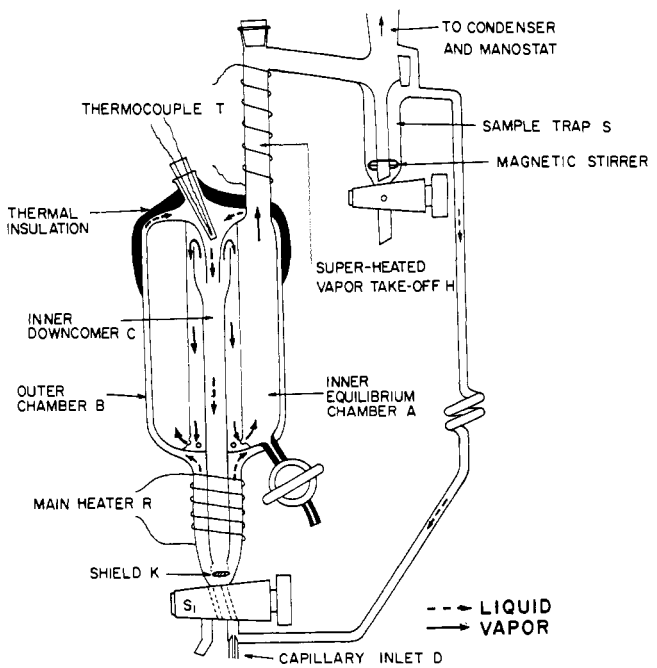

Figure 1. Equilibrium still

The most satisfactory operation of the still was experienced with a fairly low liquid level in the inner chamber. Construction of the still poses a task of moderate difficulty to an experienced glassblower. The alignment of inner and outer chambers to provide a uniform annular area with small clearance (±2 mm) requires particular attention. With its present dimensions, the still is not particularly suited to low-pressure operation, and modification of the design to reduce pressure drop along the restricted vapor path is advised for such duty.

EXPERIMENTAL

The two binary systems examined in the present study were ethanol–n-heptane and methanol–n-hexane. Heats-of-mixing data for these systems are available from the work of Van Ness and co-workers (*17, 18*). The methanol used was the 99.9 mol % Fisher Certified reagent and the n-heptane and n-hexane were Pure Grade reagents of the Phillips Petroleum Co. Ethanol was the anhydrous reagent supplied by Queen's University. Physical properties of these reagents are compared with values from the literature in Table I.

A Fisher Cartesian manostat in series with a 10-liter reservoir at constant temperature was used to control operating pressure to 760 ± 0.4 mm of mercury for both systems. Temperature measurement was estimated to be accurate to ±0.1°C. At moderate rates of circulation steady state was reached in $1^1/_2$–$2^1/_2$ hr depending on composition. Ethanol–heptane mixtures were analyzed by refractive index. Methanol–hexane mixtures were analyzed chromatographically in the range 0.10–0.92 mol fraction and by refractive index in the remaining composition intervals. Samples were dissolved in a small amount of pure benzene before chromatographic analysis to avoid phase separation.

LIQUID-PHASE ACTIVITY COEFFICIENTS

Composition-temperature data are shown in Tables II and III and Figures 2 and 3. Also shown are the liquid-phase activity coefficients. Accurate computation of the latter requires that vapor-phase nonidealities be taken into account. The corrections are conveniently incorporated in the expressions (*15*) below:

$$\ln \gamma_1 = \ln \frac{y_1 P}{x_1 P_1^0} + \frac{(B_{11} - v_1^L)(P - P_1^0)}{RT} + \frac{P y_2^2 \delta_{12}}{RT} \quad (1a)$$

$$\ln \gamma_2 = \ln \frac{y_2 P}{x_2 P_2^0} + \frac{(B_{22} - v_2^L)(P - P_2^0)}{RT} + \frac{P y_1^2 \delta_{12}}{RT} \quad (1b)$$

δ_{12} is defined in terms of the second virial coefficients:

$$\delta_{12} = 2B_{12} - B_{11} - B_{12} \quad (1c)$$

These equations are essentially rigorous if the vapor phase at all compositions is satisfactorily described by the volume-explicit virial equation of state truncated at the second virial coefficient, and if the pure component liquid molar volumes (v_1^L, v_2^L) are pressure independent over the range of interest. The magni-

Table I. Physical Properties of Materials Used

Material	$n^{20}D$	Lit. value	Normal bp	Lit. value
Ethanol	1.3620	1.3614 (*10*)	78.5	78.3 (*10*)
n-Heptane	1.3880	1.3878 (*5*)	98.4	98.4 (*5*)
Methanol	1.3290	1.3287 (*10*)	64.9	64.7 (*10*)
n-Hexane	1.3757	1.3749 (*10*)	68.1	68.7 (*10*)

Table II. Equilibrium Data and Computed Activity Coefficients for Ethanol–*n*-Heptane System at 760 Mm Hg

Mole fraction ethanol		Temp,		Correction factor, γ_1(corr)		Correction factor, γ_2 (corr)
In liquid	In vapor	°C	Ln γ_1	γ_1	Ln γ_2	γ_2
0.013	0.205	90.5	2.320	1.028	−0.002	0.986
0.023	0.330	85.0	2.422	1.019	0.003	0.977
0.025	0.360	85.6	2.402	1.019	−0.059	0.979
0.051	0.490	76.8	2.328	1.005	0.021	0.968
0.083	0.535	75.6	1.974	1.002	0.004	0.967
0.128	0.570	72.0	1.746	0.996	0.098	0.964
0.181	0.580	73.3	1.364	0.998	0.093	0.966
0.241	0.590	72.4	1.131	0.997	0.176	0.965
0.309	0.605	71.6	0.939	0.995	0.260	0.965
0.406	0.625	71.4	0.706	0.994	0.367	0.965
0.546	0.635	71.1	0.437	0.994	0.620	0.965
0.610	0.648	71.4	0.334	0.994	0.726	0.966
0.660	0.653	71.2	0.271	0.993	0.856	0.966
0.679	0.660	71.3	0.249	0.993	0.890	0.967
0.690	0.666	71.3	0.242	0.993	0.907	0.967
0.742	0.678	71.2	0.191	0.993	1.058	0.967
0.821	0.700	71.5	0.109	0.993	1.344	0.969
0.880	0.732	71.9	0.068	0.993	1.618	0.970
0.886	0.732	72.1	0.053	0.993	1.663	0.971
0.910	0.760	72.5	0.048	0.993	1.777	0.972
0.961	0.847	74.5	0.022	0.995	2.099	0.978
0.961	0.837	74.3	0.018	0.995	2.169	0.978
0.969	0.881	75.4	0.017	0.996	2.049	0.981

Table III. Equilibrium Data and Computed Activity Coefficients for Methanol–*n*-Hexane System at 760 Mm Hg

Mole fraction methanol		Temp,		Correction factor, γ_1 (corr)		Correction factor, γ_2 (corr)
In liquid	In vapor	°C	Ln γ_1	γ_1	Ln γ_2	γ_2
0.010	0.300	56.9	3.737	1.004	0.025	0.984
0.022	0.418	51.3	3.507	0.990	0.044	0.981
0.040	0.439	51.2	2.962	0.989	0.030	0.981
0.095	0.477	50.5	2.208	0.986	0.044	0.982
0.175	0.491	49.9	1.650	0.984	0.131	0.982
0.283	0.496	50.0	1.175	0.984	0.259	0.982
0.405	0.497	49.9	0.823	0.984	0.447	0.982
0.525	0.502	49.0	0.612	0.983	0.694	0.982
0.704	0.500	49.9	0.276	0.984	1.139	0.983
0.724	0.500	49.9	0.248	0.984	1.209	0.983
0.846	0.516	50.2	0.110	0.984	1.750	0.984
0.854	0.516	50.1	0.105	0.984	1.807	0.983
0.875	0.515	50.2	0.075	0.984	1.961	0.983
0.906	0.550	51.4	0.054	0.985	2.131	0.986
0.906	0.551	51.2	0.064	0.984	2.135	0.986
0.922	0.560	51.7	0.041	0.985	2.285	0.987
0.923	0.560	51.6	0.045	0.985	2.301	0.987
0.949	0.612	52.8	0.054	0.985	2.549	0.990
0.957	0.635	53.8	0.040	0.986	2.625	0.992
0.965	0.664	54.7	0.039	0.987	2.719	0.994
0.965	0.695	55.8	0.039	0.988	2.587	0.997
0.968	0.694	55.6	0.042	0.988	2.687	0.997
0.977	0.768	58.2	0.027	0.991	2.657	1.002
0.978	0.755	57.9	0.022	0.991	2.765	1.001
0.993	0.935	63.0	0.015	0.997	2.426	1.014
0.9955	0.950	63.5	0.009	0.998	2.590	1.015

tudes of the vapor-phase correction factors, γ_1 (corrected)/γ_1, are shown in Tables II and III.

The pure component vapor pressures (P_1^0, P_2^0) were computed at the experimental temperatures from Antoine-type equations using the constants given by van Ness et al. (*18*) (ethanol, heptane) and by Jordan (*8*) (methanol, hexane). Molar volumes were determined using density-temperature formulas given in International Critical Tables (*6*).

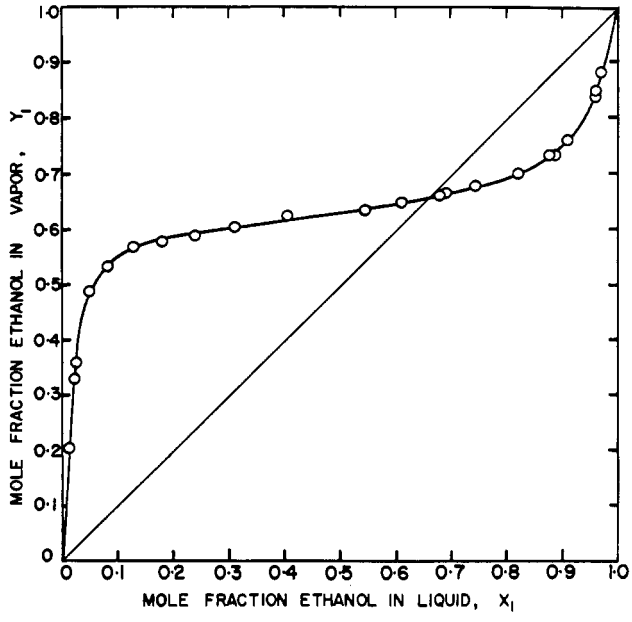

Figure 2. Phase equilibrium data for ethanol–*n*-heptane at 760 mm Hg

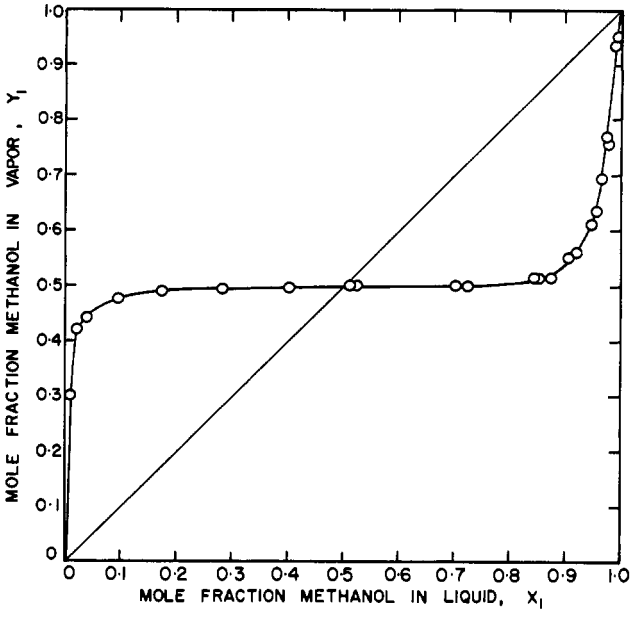

Figure 3. Phase equilibrium data for methanol–*n*-hexane at 760 mm Hg

ESTIMATION OF VIRIAL COEFFICIENTS

Second virial coefficients for ethanol and methanol were computed as functions of temperature from the recently measured values given by Knoebel and Edmister (*11*). These were fitted to equations of the form

$$B_{11} = AT^2 + BT + C$$

yielding the constants shown in Table IV. A similar procedure was followed to obtain B_{22} for heptane and hexane in the temperature range of interest based on the data of McGlashan and Potter (*12*). The corresponding constants in the above equation are also listed in Table IV.

Second virial cross coefficients B_{12} for the two systems were determined from the correlations of Pitzer and Curl (*14*), using

Table IV. Second Virial Coefficients of Pure Components as Functions of Temperature According to Equation

$$B_{ii} = AT^2 + BT + C$$

Component	Units for T	A	B	C	Source of B_{ii} data
Ethanol	°C	−0.40875	86.275	−5227.0	(*11*)
Methanol	°C	−0.84125	134.125	−6098.0	(*11*)
n-Heptane	°K	−0.08055	71.390	−16928.5	(*12*)
n-Hexane	°K	0.16932	−101.587	13643.3	(*12*)

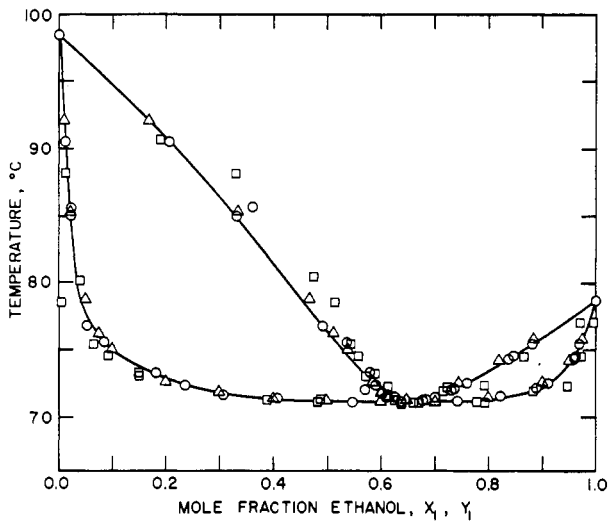

Figure 4. Temperature-composition diagram for ethanol–*n*-heptane at 760 mm Hg

△ (*18*). □ (*9*). ○ This work

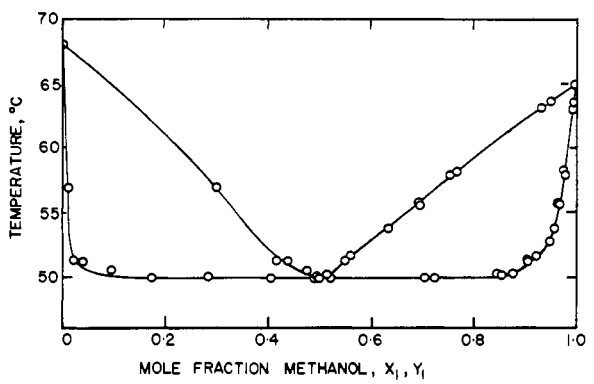

Figure 5. Temperature-composition diagram for methanol–*n*-hexane at 760 mm Hg

the "mixing rules" and acentric factors suggested by Prausnitz (*15*, *16*).

THERMODYNAMIC CONSISTENCY TESTS

Experimental temperature-composition curves for the two systems are shown in Figures 4 and 5 and are compared with the data of Katz and Newman (*9*) and those of van Ness et al. (*18*) computed from heats of mixing and P-x data. The latter data are in good agreement with those of the present study. Activity coefficients computed according to Equation 1 are shown in Figures 6 and 8. It should be noted that our results for ethanol–heptane confirm the maximum in the log γ_1 vs. x_1 curve found by van Ness et al. (but disregarded by Katz and Newman) and also show a maximum in the ln γ_2 vs. x_1 curve.

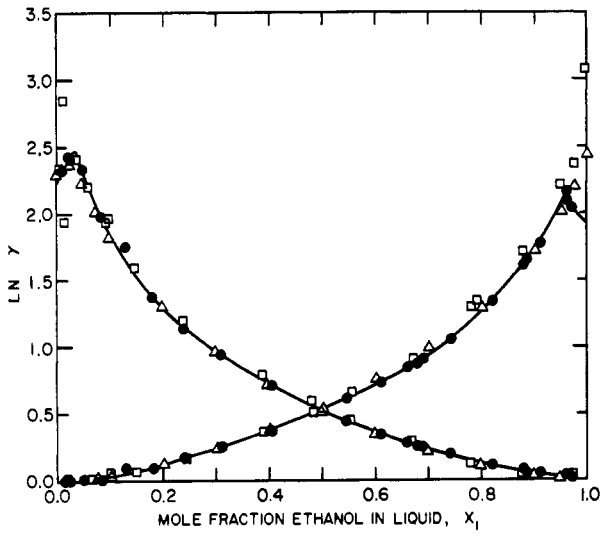

Figure 6. Corrected activity coefficients for ethanol–*n*-heptane at 760 mm Hg

△ (*18*). □ (*9*). ● This work

The availability of heat-of-mixing data for the systems investigated permits rigorous testing of the experimental data for thermodynamic consistency. For isobaric data, the requirement (*15*) is:

$$\int_0^1 \ln \frac{\gamma_1}{\gamma_2}\, dx_1 = \int_{x_1=0}^{x_1=1} \frac{\Delta H}{RT^2}\, dT \qquad (2)$$

The term $\Delta H/RT^2$ is conveniently evaluated as a function of temperature and composition from the relationship given by van Ness et al. (*18*).

$$\frac{\Delta H}{x_1 x_2 R} = AT + \frac{BT^2}{2} + \frac{DT^3}{3} + C \qquad (3)$$

For the system ethanol–heptane the "constants" (which are functions of composition) are available directly from the above work (*18*). For methanol–hexane the corresponding constants were determined by regression analysis using the experimental heat-of-mixing data of Savini et al. (*17*).

The right-hand term in Equation 2 was evaluated by numerical integration, using Lobatto's method, of the curves shown in Figures 7 and 8. The first term in Equation 2 was evaluated

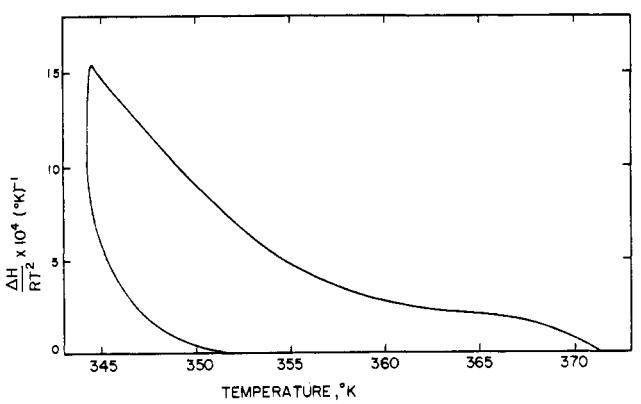

Figure 7. Heat-of-mixing data as function of temperature for ethanol–*n*-heptane

Data by Van Ness et al. (*18*)

Table V. Thermodynamic Consistency Tests

System	$\int_{x=0}^{x=1}(\Delta H/RT^2)dT$ (= A_H)	$\int_0^1 \ln \gamma_1 dx_1$ (= A_1)	$\int_0^1 \ln \gamma_2 dx_1$ (= A_2)	ΔA (= $A_1 - A_2 - A_H$)	$\int_0^1 \ln \frac{\gamma_1}{\gamma_2} dx_1 - A_H$	ΣA	$\frac{\Delta A}{\Sigma A}$ Cor	$\frac{\Delta A}{\Sigma A}$ Uncor
Ethanol–*n*-heptane	0.0227	0.7338	0.6980	0.0131		1.4545[a]	0.0090	0.0306
					0.0075[b]	1.0449[c]	0.0072	
Methanol–*n*-hexane	0.0009	0.9022	0.8537	0.0476		1.7568[a]	0.0270	0.0273
					0.0435[b]	1.2556[c]	0.0348	

[a] $\Sigma A = A_1 + A_2 + A_H$. [b] From a plot of $\ln \gamma_1/\gamma_2$ vs. x_1. [c] $\Sigma A = A_H + \int_0^{x_0} \ln \gamma_1/\gamma_2\, dx_1 - \int_{x_0}^1 \ln \gamma_1/\gamma_2\, dx_1$ (x_0 = point where $\gamma_1 = \gamma_2$).

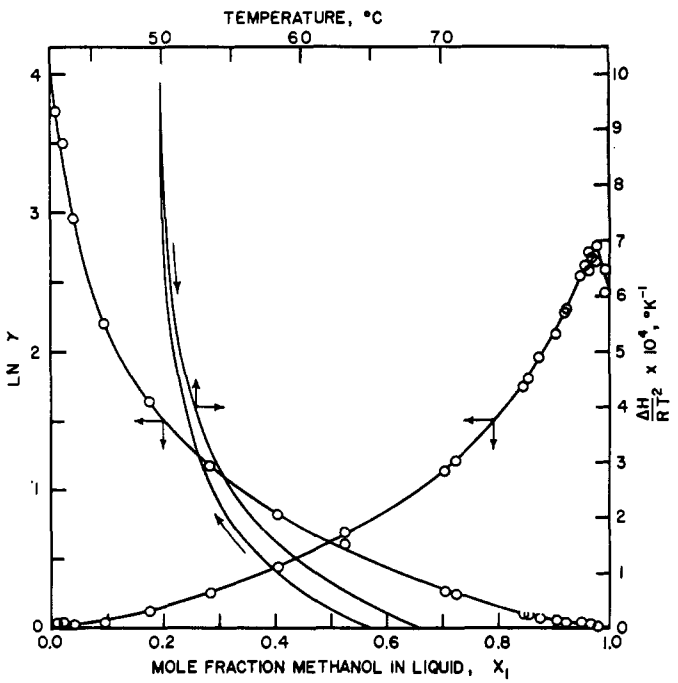

Figure 8. Corrected activity coefficients for methanol–n-hexane at 760 mm Hg

$\Delta H/RT^2$ curve based on data by Savini et al. (17)

by numerical integration, using Simpson's rule, of the plots shown in Figures 6 and 8. As a check, the area under the curve in a plot of $\ln \gamma_1/\gamma_2$ vs. x_1 was similarly evaluated. The results of these tests are shown in Table V. Also included are results obtained with uncorrected activity coefficients (i.e., coefficients computed using only the second term in Equation 1).

Although the possibility of compensating errors in an integral test cannot be discounted, results of the test for the ethanol–heptane system suggest that the data are remarkably consistent. The consistency indicated by the result

$$\frac{\Delta A}{\Sigma A} \leq 0.009 \tag{4}$$

for example, is well inside the criterion

$$\frac{\Delta A}{\Sigma A} \leq 0.02 \tag{5}$$

proposed by Prausnitz (*15*) "for systems of moderate nonideality."

Data for the system methanol–*n*-hexane are less consistent. In the very dilute region $x_1 < 0.05$, the relative volatility of methanol is extremely large (e.g., $\alpha^{12}_{x_1=0.01} > 40$) and accurate determination of equilibrium data in this region poses a considerable challenge. The temperature recorded at steady state for the experimental point $x_1 = 0.01$ showed a rapid uniform oscillation of small amplitude about the mean value of 56.9°C. This suggests that, with the exceptionally large differences in vapor and liquid compositions, mixing in the outer chamber in the region above the stopcock, S_1, may have been incomplete, possibly leading to some error in the *T-x-y* curves for the very dilute region. Small experimental error in this region may appreciably influence the integral

$$\int_0^1 \ln \gamma_1 dx_1 \left(\text{or } \int_0^1 \ln \frac{\gamma_1}{\gamma_2} dx_1\right)$$

as seen from Figure 6. Additional mechanical stirring in the lower portion of the outer chamber seems advisable for conditions of such extreme temperature–composition sensitivity.

The maxima observed in the $\ln \gamma_i$ vs. x_i curves for both systems indicate that in certain regions the quantity

$$x_i \frac{d \ln \gamma_i}{dx_1} + \frac{\Delta H}{RT^2}\frac{dT}{dx_1} \tag{6}$$

changes sign owing to the extraordinary steepness of the temperature gradients (evident from the Gibbs-Duhem equation for constant pressure:

$$x_1 \frac{d \ln \gamma_1}{dx_1} = -x_2 \frac{d \ln \gamma_2}{dx_1} - \frac{\Delta H}{RT^2}\frac{dT}{dx_1}\Big)$$

CONCLUSIONS

Equilibrium data presented for the two alcohol–hydrocarbon systems have been shown to have high thermodynamic consistency. The results suggest that the proposed equilibrium still is capable of producing accurate data for very demanding nonideal systems. For highest accuracy with systems (or in composition regions) where relative volatility is extremely large, incorporation of an additional stirring device in the lower region of the outer chamber is advised.

ACKNOWLEDGMENT

The authors are indebted to Carl Levay for his expert assistance in the construction of the still.

NOMENCLATURE

A, B, C, D = constants in Equation 3 or in the equation for $B_{ii} = f(T)$

$A_1 = \int_0^1 \ln \gamma_1 dx_1$

$A_2 = \int_0^1 \ln \gamma_2 dx_1$

$A_H = \int_{x=0}^{x=1} (\Delta H/RT^2) dT$

$\Delta A = A_1 - (A_2 + A_H)$

ΣA = area sum as defined in Table V

B_{11} = second virial coefficient for pure component 1

B_{22} = second virial coefficient for pure component 2

B_{12} = second virial cross coefficient

ΔH = molar enthalpy of mixing, J/g mol

P = total pressure

P_1^0, P_2^0 = vapor pressures of pure components 1, 2

R = gas constant

T = temperature, °K

v_1^L, v_2^L = pure component liquid molar volumes, cc/g mol

x_1, x_2 = mole fractions of components 1, 2 in liquid phase

y_1, y_2 = mole fractions of components 1, 2 in vapor phase

GREEK LETTERS

α^{12} = relative volatility

γ_1, γ_2 = liquid-phase activity coefficients of components 1, 2

$\delta_{12} = 2B_{12} - B_{11} - B_{22}$

SUBSCRIPTS

1 = component 1

2 = component 2

i = component 1 or component 2

LITERATURE CITED

(1) Brown, I., *Austr. J. Sci. Res., Ser. A; Phys. Sci.*, **5** (3), 530 (1952).

(2) Fowler, R. T., Morris, G. S., *J. Appl. Chem. (London)*, **5**, 266 (1955).

(3) Gillespie, D. T. C., *Ind. Eng. Chem., Anal. Ed.*, **18**, 575 (1946).

(4) Hala, E., Pick, J., Fried, V, Villim, O., "Vapor-Liquid Equilibrium," 2nd ed., p 280, Pergamon Press, New York, N.Y., 1967.

(5) "Handbook of Chemistry and Physics," 50th ed., p C321, Chemical Rubber, Cleveland, Ohio, 1969.

(6) "International Critical Tables," Vol. 3, pp 27, 29, McGraw-Hill, New York, N.Y., 1929.

(7) Jones, C. A., Schoenborn, E. M., Colburn, A. P., *Ind. Eng. Chem.*, **35**, 666 (1943).

(8) Jordan, T. E., "Vapor Pressure of Organic Compounds," pp 6, 65, Interscience, New York, N.Y., 1954.

(9) Katz, K., Newman, M., *Ind. Eng. Chem.*, **48**, 137 (1956).

(10) "Kirk Othmer Encyclopedia of Chemical Technology," 2nd ed., Vol. 8 p 42; Vol. 11, p 1; Vol. 13, p 370, Interscience, New York, N.Y., 1965.

(11) Knoebel, D. H., Edmister, W. C., *J. Chem. Eng. Data*, **13**, 312 (1968).

(12) McGlashan, M. L., Potter, D. J. B., *Proc. Roy. Soc.*, **267A**, 478 (1962).

(13) Otsuki, H., Williams, C. F., *Chem. Eng. Progr. Symp. Ser.*, **49** (6), 55 (1953).

(14) Pitzer, K. S., Curl, R. F., *J. Amer. Chem. Soc.*, **79**, 2369 (1957).

(15) Prausnitz, J. M., "Molecular Thermodynamics of Fluid-Phase Equilibrium," pp 74, 157, 214, 471, Prentice-Hall, Englewood Cliffs, N.J., 1969.

(16) Prausnitz, J. M. Eckert, C. A., Orye, R. V., O'Connell, J. P., "Computer Calculations for Multicomponent Vapor-Liquid Equilibria," p 20, Prentice-Hall, Englewood Cliffs, N.J., 1967.

(17) Savini, C. G., Winterhalter, D. R., Van Ness, H. C., *J. Chem. Eng. Data*, **10**, 168 (1965).

(18) Van Ness, H. C., Soczek, C. A., Kochar, N. K., *ibid.*, **12**, 346 (1967).

RECEIVED for review January 28, 1971. Accepted November 1, 1971. Paper presented at the Chicago meeting of the AIChE, 1970. This work was supported in part by grants from the National Research Council of Canada.

Emf Measurements in Additive Ternary Molten Salt Systems $PbCl_2$–KCl–NaCl and $PbCl_2$–CsCl–NaCl

KJELL HAGEMARK,[1] DENNIS HENGSTENBERG, and MILTON BLANDER[2]

North American Rockwell Science Center, Thousand Oaks, Calif. 91360

Emf measurements in the binary molten systems, $PbCl_2$–NaCl, $PbCl_2$–KCl, and $PbCl_2$–CsCl, and in the ternary systems, $PbCl_2$–NaCl–KCl and $PbCl_2$–NaCl–CsCl, were made at mole fractions of $PbCl_2$ of 0.5 and 0.3. Our data (as well as some previous data) on excess free energies of solution in the three binary systems are consistent with the equation first suggested by Førland (Equation 1) in terms of equivalent fractions, with the coefficients λ = −1800, −10,300, and −15,500 cal/mol for the mixtures with NaCl, KCl, and CsCl, respectively. Measurements of $\bar{G}_{PbCl_2}^E$ at constant mole fractions of $PbCl_2$ in the ternary systems exhibited small negative deviations from additivity.

In this paper we present electromotive force measurements and partial molar quantities for $PbCl_2$ in the three binary systems $PbCl_2$–NaCl, $PbCl_2$–KCl, and $PbCl_2$–CsCl, and in the two ternary systems, $PbCl_2$–NaCl–KCl and $PbCl_2$–NaCl–CsCl, at mole fractions of $PbCl_2$ of 0.5 and 0.3. A critique of previous work on the binary systems is given, and we show that the simplest representation of the data on the activity coefficients, γ, and the partial molar excess free energy, $\bar{G}^E$, of $PbCl_2$ has a form first suggested for the binaries by Førland (*2*, *6*):

$$\bar{G}_{PbCl_2}^E = RT \ln \gamma_{PbCl_2} = \lambda(1 - N_{PbCl_2}')^2 \qquad (1)$$

[1] Present address, 3M Central Research Laboratory, St. Paul, Minn. 55119

[2] Present address, Chemical Engineering Division, Argonne National Laboratory, Argonne, Ill. 60439. To whom correspondence should be addressed.